Emergent Materials
https://doi.org/10.1007/s42247-025-01024-9

ORIGINAL ARTICLE

Utilization of polyethylene waste for designing foamy oil sorbents

Sarah M. Hailan[1,2] · Zuzana Nogellova[3] · Anton Popelka[1] · Marketa Ilcikova[4,5] · Miroslav Mrlík[4] · Antonín Minařík[4,5] · Filip Mikulka[5] · Gordon McKay[1] · Igor Krupa[2,6]

Received: 12 October 2024 / Accepted: 27 January 2025

Abstract
Recycling low-density polyethylene (LDPE) in its original form presents several challenges, including limited interest from converters, poor market demand for recycled products, higher sorting and cleaning costs, and reduced quality in the final products. It happens because recycled LDPE often exhibits lower mechanical strength and diminished aesthetic appeal than its virgin counterpart, making it rarely suitable for its original purpose, especially in packaging. Therefore, new applications for LDPE recyclates are needed to overcome these barriers and extend the material's lifecycle. One such solution involves converting LDPE waste into foamy sorbents for water purification. The presented study investigated two strategies for recycling LDPE waste by exploring the potential of the modified waste to remove free oil spills. The first approach involves preparing and characterizing robust, mechanically stable foams using recycled waste from LDPE packaging. The process is based on parallel foaming and crosslinking of LDPE by peroxides. The final foamy structure (Foam 1) possesses around 75 vol% of pores (46 vol% open pores) and rapidly absorbs various organic liquids quickly (hexane, diesel oil, crude oil) in multiple cycles. The second target deals with the screening, testing, and characterizing of LDPE-based foams that were initially used for various packaging and deposited as waste to explore their potential free oil sorbents. The foam that was used in this study has a significantly porous structure, having 96 vol% of pores and more than 89 vol% open pores (Foam 2). Whereas the sorption capacity of Foam 1 was 4–5 g/g, depending on the type of oil, Foam 2 absorbed those oils in the range of 8–12 g/g. The Foam 1 showed significantly better stability over multiple cycles and better mechanical performance.

Keywords LDPE · Recycling · Foams · Oil removal · Absorption

1 Introduction

Polyethylene, PE, the most widely used synthetic polymer, predominantly in packaging, generates the largest share of plastic waste [1]. Packaging alone accounts for about 46% of plastic waste [1, 2]. However, recycling plastic, mainly low-density polyethylene (LDPE), is associated with big challenges. These issues include low demand from converters, the limited market appeal of recycled products, higher costs regarding sorting and cleaning, lowered quality and mechanical behavior, and poorer aesthetic performance compared to neat materials [3]. New utilization of LDPE recyclates originating from various sources, particularly packaging, is required to address these challenges, extending the lifespan of plastics. This problem is even more challenging when LDPE is involved in multilayered packaging, such as TetraPak. In this case, LDPE/Aluminium bilayers are hardly separable and need special attention for practical

✉ Igor Krupa
igor.krupa@qu.edu.qa

1 Division for Sustainable Development, College of Science and Engineering, Hamad bin Khalifa University, Qatar Foundation, Education City, Doha, Qatar

2 Center for Advanced Materials, Qatar University, Doha 2713, Qatar

3 Polymer Institute, Slovak Academy of Sciences, Dubravska cesta 9, Bratislava 84541, Slovakia

4 Centre of Polymer Systems, Tomas Bata University in Zlin, Trida T. Bati 5678, Zlin 760 01, Czech Republic

5 Department of Physics and Materials Engineering, Faculty of Technology, Tomas Bata University in Zlin, Vavřečkova 275, Zlin 70 01, Czech Republic

6 Materials Science and Technology Graduate Program, College of Arts and Sciences, Qatar University, Doha 2713, Qatar

Published online: 04 February 2025

recycling [4]. One of the perspective options seems to be transferring polyethylene waste into sorbents applicable for oil/water separation. This approach includes powdered adsorbents for oil purification in oil-water emulsions [5, 6] and PE-based foams and mats that efficiently absorb free oil spills [7]. Oil removal is a critical water treatment component, particularly for managing oil spills and treating contaminated wastewater [8, 9].

While 3D polymer structures like foams, sponges, and wools made from polyethylene are less commonly used for oil sorption, materials such as polydimethylsiloxane [10], melamine [11], and polyurethane foams [12] are favored due to their significantly higher sorption capacities. These materials allow easy oil recovery through squeezing, making them reusable [13, 14]. Additionally, these advanced sorbents offer key advantages, including customizable wettability, environmental safety, and scalability.

Polyolefin-based sorbents offer a promising approach to water purification by addressing plastic waste accumulation while harnessing the beneficial properties of polyolefins for this purpose [15, 16].

Commercial LDPE foams are primarily used for packaging and insulation. They can have various densities, porosities, formulations, and designs. Mostly, they are closed-cell foam. It provides resistance to water and strength and rigidity that are not present in open-cell foams. For example, an open pore structure can be formed by supercritical CO_2 foaming. Binbin Sun et al. [17] prepared highly open-porous foams from ultra-high molecular weight PE (UHMWPE). They were applied to remove various organic liquids (methyl alcohol, chloroform, ethanol, hexane, xylene, dichloromethane). The observed fast sorption with absorption capacity ranges from 4 to 10 g/g, depending on the type of liquid. Foams also showed excellent stability and high absorption capacity over ten cycles. Similarly, Su et al. [18] created UHMWPE foams by dissolving the polymer in p-xylene and freeze-drying the solution under vacuum conditions. The foams' absorption capacities ranged from 28 to 85 g/g for cyclohexane and carbon tetrachloride. An interesting porous structure on the base of linear LDPE was studied by Nam et al. [19–21]. They explored the preparation, characterization, and large-scale potential of polyethylene-based porous networks, known as i-Petrogel, which exhibit a high sorption capacity for organic liquids. The study involved linear low-density polyethylene (LLDPE) crosslinked by poly(1-decene-co-divinylbenzene) copolymer [19–21]. These materials can absorb a wide range of organic solvents and oils, with capacities reaching up to 40 g/g.

Recently, Sun et al. [22] developed an ultra-lightweight foam based on UHMWPE and high-density polyethylene (HDPE) using microcellular foaming technology. The composites were prepared by hot-melt blending the components in various ratios at 190 °C, followed by hot pressing at the same temperature. Foaming was performed by CO_2. The absorption capacity of the foam was 9.8 g/g for cyclohexane and 15 g/g for carbon tetrachloride. In another paper, Sun et al. [23] graphite nanoplatelets (GNPs) were added to UHMWPE by melt blending, then foaming the composite using supercritical CO_2 microcellular foaming technology. Adding GNPs enhanced the cell growth and expansion rate of UHMWPE. However, this study focuses on utilizing LDPE waste to remediate free oil spills. The first target involves preparing and characterizing robust, mechanically stable foams using recycled waste from LDPE packaging. The second is a screening, testing, and characterization of polyethylene foams initially used for various packaging and discarded as waste to explore their potential free oil sorbents.

2 Experimental

2.1 Materials

Foams were prepared from recycled LDPE from Twyla (Qatar). LDPE has a specific density of 0.915 g/cm³, a melting point of 108.2 °C, and a specific enthalpy of melting of 45 J/g. The blowing agents (BA) were composed of 1,1′-azobiscarbamide, including Genitron AC2 (Schering Polymer Additives, UK), PB-20, and MB-1000 (Hangsun Plastic Additives Co. Ltd., China). Crosslinking was achieved using 2,5-dimethyl-2,5-di-(tert-butylperoxy)hexyne-3 (Luperox130, Arkema, France) and dicumyl peroxide (DCP, Sigma-Aldrich, USA). LDPE, BA, and crosslinking agents (XA) were blended in various ratios for 10 min at 140 °C in a Plastograph (Brabender GmbH & Co. KG, Duisburg, Germany). The BA content was 5, 7.5, 10, and 15 phr (grams of BA per 100 g of a mixture), and the XA content was 0.5, 0.75, 1, 1.5, and 2 phr (grams of XA per 100 g of a mixture). The mixtures were hot-pressed in a cylindrical mold at 160 °C for 3 min. This step was followed by an additional heating step at 180 °C for 13 min to promote crosslinking. Lastly, the sample was placed in an oven and maintained at 180 °C for 25 min to decompose the BA, forming the foamy material. Compositions and morphologies of some foams are shown in S1. Foams were first characterized visually by an optical microscope and by determination of specific densities. Foam #5 (S1) was used to test oil sorption performance. It was prepared using AC 2 blowing agent (10 phr) and 1 phr of DCP Fig. 1.

For a comparison, apart from newly prepared foams from recycled LDPE, we also tested polyethylene foam collected from waste that initially served as a packaging material for a computer.

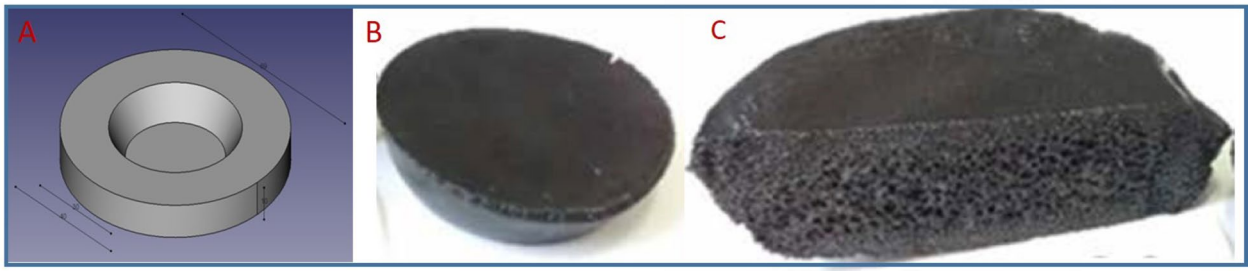

Fig. 1 The shaping form (**A**), the sample before foaming in an oven (**B**), and a prepared Foam 1 (**C**)

Absorption experiments were performed using hexane (dynamic viscosity: 0.31 mPa·s; specific density: 0.660 g/cm³), diesel oil (dynamic viscosity: 3.4 mPa·s; specific density: 0.850 g/cm³), and crude oil (dynamic viscosity: 12 mPa·s; specific density: 0.990 g/cm³,). All these values were measured at a temperature of 20 °C.

2.2 Absorption test

Absorption tests were done using cuboid samples measuring 1.5 × 1.5 × 0.1 cm. These samples were immersed in a selected oil at a temperature of 22 °C, and their mass was recorded at predetermined intervals. Each test was repeated three times to ensure reliability, and the collected data were utilized to analyze the absorption kinetics. Multiple sorption and desorption experiments tested the reusability of the foam were performed. In these tests, the foams were submerged in oil for one hour, after which the oil was manually squeezed. The foams were then re-immersed in oil without any prior cleaning or treatment, and this cycle was repeated ten times. The oil was manually extracted from the saturated samples by squeezing them in a syringe. It ensured a constant deformation across all samples.

The porosity of the samples was assessed using a disk-shaped cut measuring 5 mm in diameter and 10 mm in height. The measurement was done by computer microtomography (CT) using a SkyScan Unit (Model 1174, Bruker, New York, NY, USA). The unit was equipped with an X-ray source operating between 20 and 50 kV at a maximum power of 40 W and an X-ray detector (Bruker, New York, NY, USA). A CCD 1.3 Mpix unit was coupled to a scintillator via a lens with a 1:6 zoom range. Projection images were recorded at angular increments of 0.3° with a tube voltage set at 31 kV and a current of 529 µA. Each exposure lasted for 10 s. Three-dimensional reconstructions were created using the preinstalled CT image analysis software (e v1.16.4.1, Bruker, New York, NY, USA). Moreover, the pore size distribution was investigated from the foam cross-sections using an Eclipse 55i optical microscope (Nikon, Japan) equipped with an EOS 200D camera (Canon, Japan). Porosity analysis was performed using ImageJ software version 1.5 (W. Rasband, National Institute of Health, United States). The acquired photo was contoured to grayscale and then converted to binary format. The "Set scale" function adjusted the photo size from pixels to micrometers. The "Analyze particles" function was used in this modified photo, and the analysis results were displayed using a histogram and a distribution curve.

2.3 SEM analysis

The morphology of the foams was visualized and examined using a Nova Nano SEM 450 scanning electron microscope (SEM, Osaka, Japan) operating at 20 kV.

2.4 Wettability measurement

The surface wettability of foams was characterized using the OCA35 optical system (Data Physics, Filderstadt, Germany) through the sessile drop technique. Distilled water, hexane, diesel, and crude oil were the testing liquids. Experiments were conducted under atmospheric and submerged environments (crude oil). A volume of 1 µL of each liquid was deposited, and the results were averaged from six independent measurements to ensure statistical reliability.

2.5 Mechanical properties

In compression mode, dynamic mechanical properties were characterized using a dynamic mechanical analyzer (DMA 1, Mettler Toledo, Switzerland). Measurements were conducted at a frequency of 1 Hz, with deformation levels ranging from 1 to 90%, all at room temperature. The compact rheometer Physica MCR-502 (Anton Paar, Austria) was employed for the compression test. The typical stress-strain experiments in compression mode have been applied, where the initial sample was in the form of a cylinder with a diameter of 10 mm and 12 mm in height. The Peltier geometry was used with upper cell PP10. The measurements were

performed at 25 °C. The initial pre-stress of 0.02 N was used to make initial contact between the geometry and the sample.

2.6 Thermogravimetry (TG)

The thermal stability of the composite was determined by carrying out a thermogravimetric analysis (TGA) from room temperature to 600 °C with a heating rate of 10 °C/min in a nitrogen atmosphere using a TGA 4000 (PerkinElmer, USA) analyzer.

3 Results and discussion

3.1 Characterization of crosslinking efficiency

Crosslinking is crucial for ensuring the stability of the final foamy structure. It helps prevent pore collapse during the foaming process and guarantees that the final product possesses the desired mechanical strength. The various peroxide concentrations were tested to evaluate crosslinking efficiency before foaming. This efficiency was assessed in terms of the insoluble (gel) content. The gel content (g) was quantitatively determined through gravimetric analysis after 24 h of extracting samples in boiling xylene, as outlined in Eq. (1). Three samples were analyzed for gel content determination, with the xylene being refreshed every six hours.

$$g = \frac{m_{extr}}{m_0} \times 100\% \tag{1}$$

where m_{extr} [g] represents the mass of the sample after extraction, while m_0 [g] denotes the initial mass of the sample.

It was found that 1 phr of peroxide led to the gel content formation of 98 wt%, indicating a highly crosslinked structure.

3.2 Morphology and porosity of the foams

The porosity of both foams was first estimated from the specific density measurements according to Eq. (2). The specific density of air was neglected, and $\rho_{LDPE} = 0.919$ g.cm^{-3}.

$$\phi_{pores} \approx 1 - \frac{\rho_{foam}}{\rho_{LDPE}} \tag{2}$$

The cube size (2 × 2 × 2 cm) and the mass determined the related densities. The specific densities were 0.230 ± 0.02 g.cm^{-3} for Foam 1 and 0.033 ± 0.001 g.cm^{-3} for Foam 2. The pore volume contents calculated from Eq. (2) are 0.75 for Foam 1 and 0.96 for Foam 2. These values give a total pore volume accounting for open and closed pores. Deeper insight into the foam porosity was performed using computer tomography, which enables the direct determination of the open pores within structures. As shown in Fig. 2, Foam 1 has a significantly porous structure with more than 89% of the open pores and a high roughness factor. On the other hand, Foam 1 showed a different structure, and the open pores were only 46%. The surface is more compact with considerably lower roughness, as confirmed by other investigations.

The pore size distribution investigation (Fig. 3) proved that most pores of Foam 2 (Fig. 3a) range from 1800 µm to 2000 µm and show an overall porosity of 90.8%. However, in the case of foam 1(Fig. 3b), most pores start from 1200 µm to 1800 µm, indicating a broader pore size distribution with overall porosity. Generally, the pores are spherical and oval, according to the images in Fig. 3a and b insets.

3.3 Surface wettability

The rates at which oil and water are absorbed play a crucial role in the oil/water separation process, as only the oil component must be absorbed while minimizing or eliminating water sorption. This behavior is influenced by the

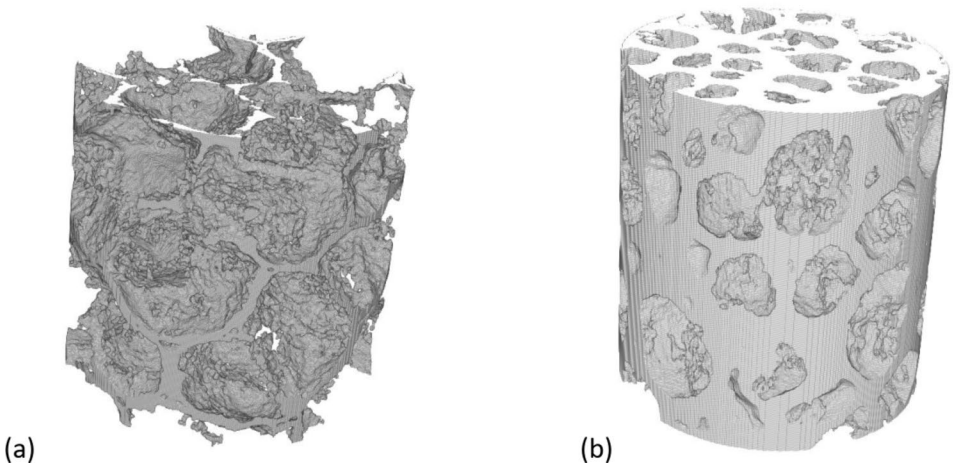

Fig. 2 The real-time reconstruction of the foam structure using computer tomography where (**a**) is Foam 2 and (**b**) is Foam 1. The diameter of the investigated structure was 5 mm, and the height was 10 mm

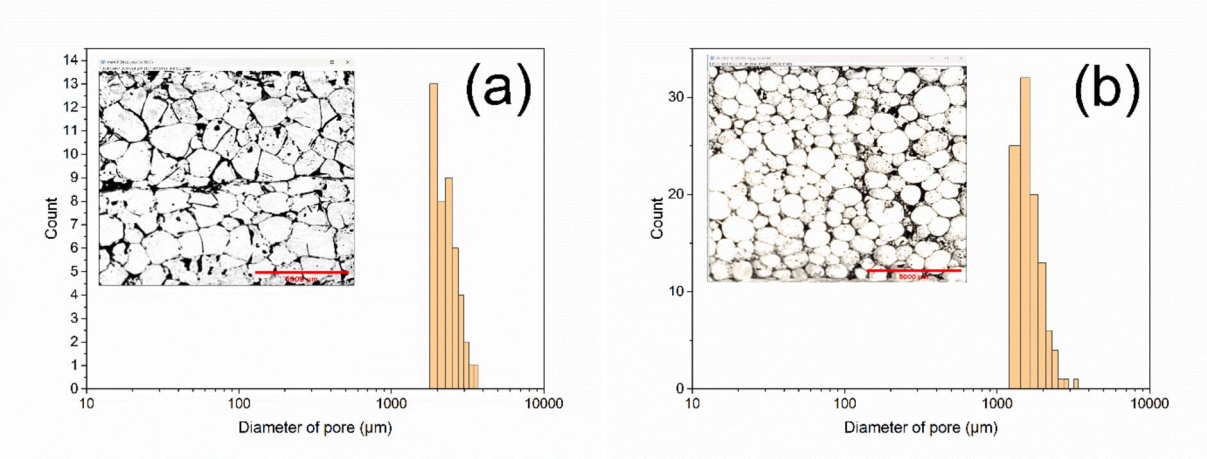

Fig. 3 Pore size distribution of Foam 2 (**a**) and Foam 1 (**b**) where figure insets are eclipse optical microscopy images of the corresponding foams. The scale bar in the figure insets is 5000 μm

wettability of the sorbent surfaces toward both water and oil [24, 25], which is typically assessed through contact angle measurements for liquids with varying polarities. The contact angle is affected by the material's chemical composition, surface roughness, and morphology [26, 27]. In this context, the contact angles of crude oil and water determine the wettability of the foams. Both foams rapidly absorbed all the oil, resulting in a zero contact angle. Different behaviors were observed when water was used to wet the foams. PE is an inherently hydrophobic material due to its nonpolar character, having a contact angle for distilled water (WCA) around 90° [28]. Chemical and physical modifications of smooth PE surface can lead to the significantly enhanced hydrophobicity characterized by high WCA [28].

The WCA of 133 ± 3° confirmed the hydrophobic character of Foam 1. Correctly determining WCA for Foam 2 is more complicated due to the roughness and surface heterogeneity [29, 30]. These factors strongly influence the measured value, which was estimated as 71 ± 3° Fig. 4.

3.4 Thermogravimetric analysis (TGA)

TGA was performed to characterize the foams' thermal stability, as shown in Fig. 5. Except for both foams, the original material used to prepare Foam 1 was tested (r-LDPE). As for Foam 2, because it was not prepared by our team and was selected as an example of foam from packaging waste, we do not have the original, neat material used for this foam preparation. The TG characterization indicates the following:

i) The thermal stability of Foam 1 is higher than the thermal stability of Foam 2. These may have two reasons. Firstly, the neat LDPE used for the preparation of Foam 1 has a higher molar mass than the LDPE used for the preparation of Foam 2, or the thermal stabilization of the former is more efficient than the latter.
ii) A comparison of the neat LDPE (marked as r-LDPE) and the prepared Foam 1 shows that the former's thermal stability is higher than the latter. This effect is probably caused by the additives (foaming agent a peroxide) used for foaming. It is also observed that Foam 1 contains some substances incorporated within the Foam 1 structure. These compounds are released when the Foam 1temperature reaches around 250°C. These compounds (rich in oxygen) also probably enhance the degradation process of Foam 1. Nevertheless, both foams are sufficiently stable up to 250°C for their use as oil sorbents.

3.5 Kinetics of absorption

The dependence of the absorption capacities (M_t) of Foam 1 and 2 on the sorption time for hexane, diesel oil, and crude oil are shown in Figs. 6 and 7, and 8. The experimental data are evaluated against specific models, as detailed in the following sections.

In all cases, we observed very rapid sorption of all oils into both foams, and the M_t dependences reached an apparent plateau in 10–20 s. These extremely high sorption rates are generally more common for highly porous melamine and polyurethane foams [11] rather than foamed thermoplastics [16, 17].

The reason for such fast sorption is the presence of the interconnected open pores with a suitable size and tortuosity within a foamed structure [31].

Different kinetic models have often been tested to describe the experimental time dependences of free oils sorption by porous structures [32–34]. The pseudo-first-order (PFO) [32] and pseudo-second-order (PSO) [33]

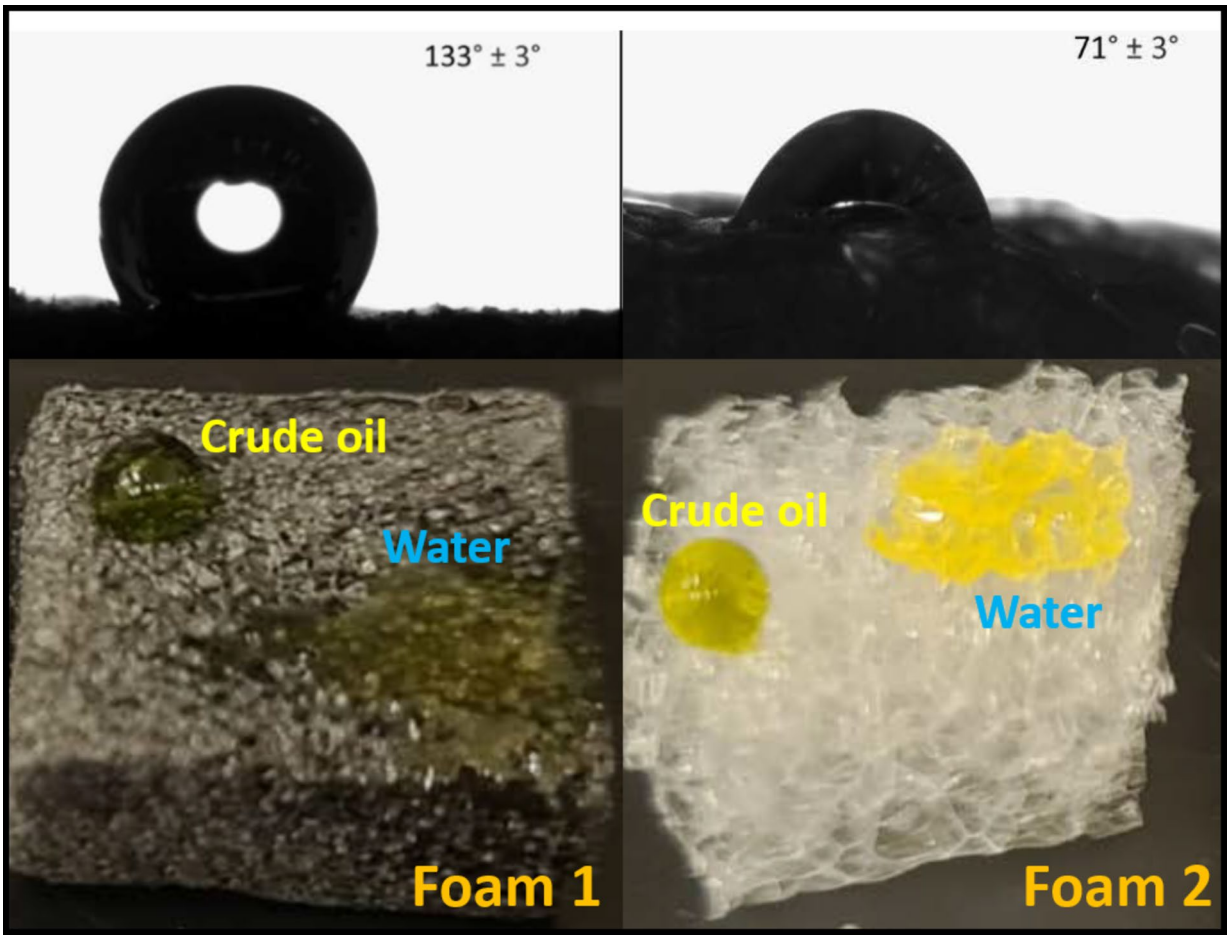

Fig. 4 Wettability of foams by water and crude oil. Water and crude oil were colored for better visibility

models are commonly employed to describe oil sorption in porous materials. These models can often effectively fit experimental sorption data [35–37]. However, their relevance for describing sorption processes is somewhat disputable because the diffusional process cannot be neglected. As recently discussed by Azizian [38], it may only be a coincidence based on the shape similarity of the curves, and fitting parameters may have a questionable physical meaning. Azizian et al. [38] proposed the so-called 'fractal-like linear driving force (FL-LDF)' model (Eq. (3)) to describe the sorption of liquids into porous substrates.

$$M_t = M_{max}[1 - \exp(-D\prime\, t^{\alpha})] \tag{3}$$

where m_t [g/g] represents the mass of liquid absorbed per mass of sorbent, while m_{max} [g/g] denotes the maximum mass of liquid absorbed per mass of sorbent. The mass transfer coefficient as indicated by D' [time$^{-\alpha}$] is the mass transfer coefficient, t [s, min] refers to the duration of the experiment, and α [-] is dimensionless fractal constant ($0<\alpha\leq1$).

The comparisons of results with the FL-LDF model are shown in Figs. 6 and 7, and 8, and the parameters D' and α are summarized in Tables 1 and 2. The model fits all the data with an appropriate accuracy.

Another model utilized is the generalized non-Fickian diffusional model, first introduced by Ritger and Peppas [39, 40]. This model interprets the non-Fickian drug release from moderately swelling polymeric structures, as represented in Eq. (4).

$$\frac{M_t}{M_\infty} = kt^n \tag{4}$$

In the original studies, M_t and M_∞ represent the mass concentrations of a released species at a given time, t and as time approaches infinity, respectively. The constant k incorporates characteristics of both the network (medium) and the species, while n denotes the diffusional exponent. When $n = 1/2$, the model depicts Fickian diffusion, which occurs in homogeneous systems without boundaries - such as pores, swollen and dry regions, and areas with varying physical states (e.g., glassy or rubbery). However, the infiltration of

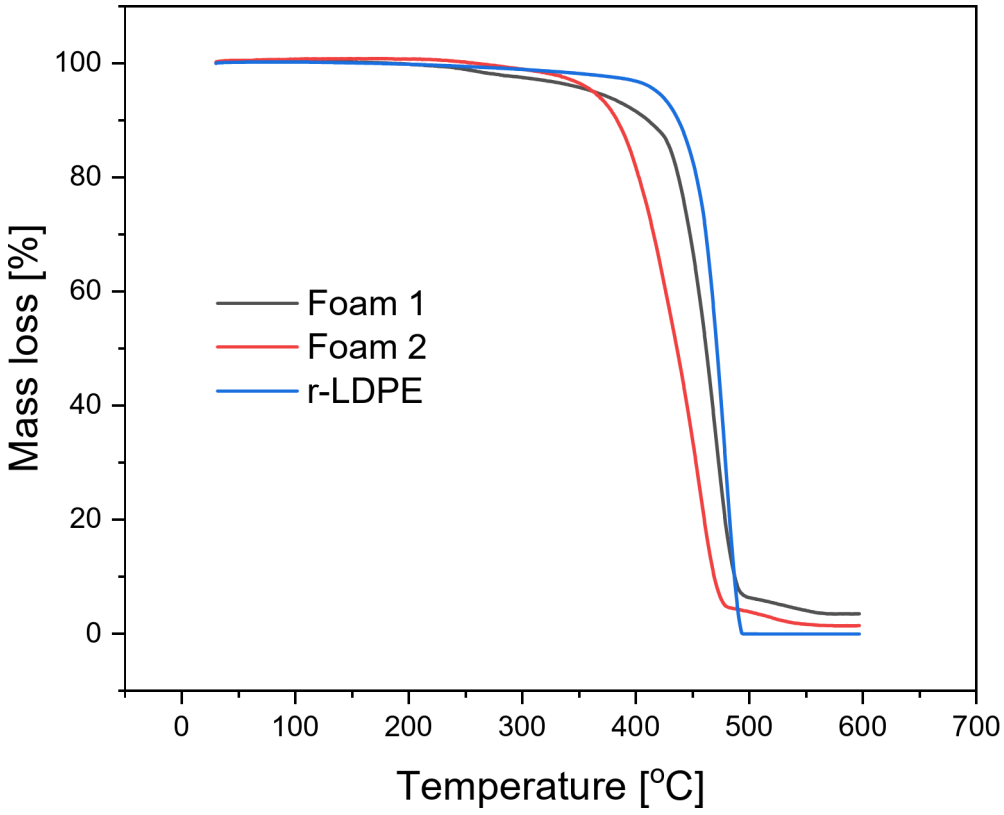

Fig. 5 TG curves of Foam 1, Foam 2, and r-LDPE

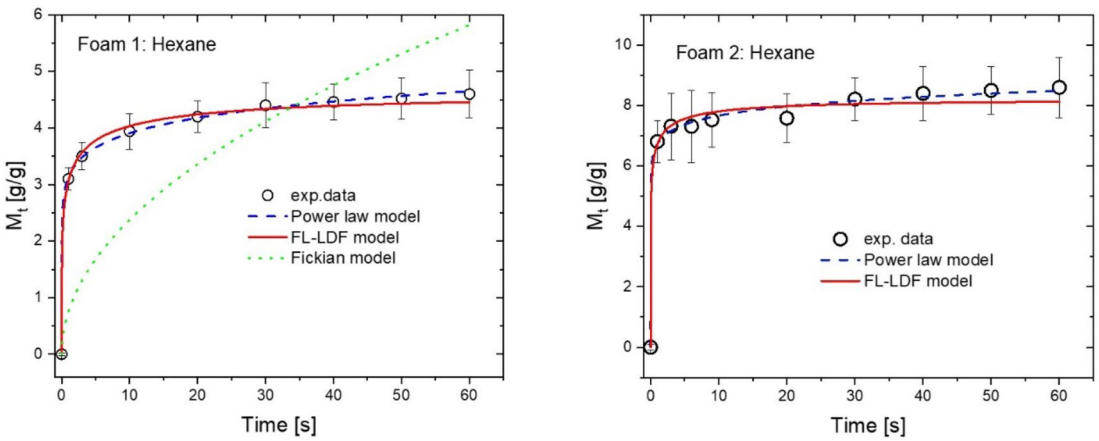

Fig. 6 Absorption capacity (M_t) of Foam 1(left) and Foam 2 (right) for hexane compared with the Power law model (blue dashed) (left), FL-LDF model (red), and Fickian model (green dotted)

liquids into foams deviates significantly from Fickian diffusion [39, 40], as evidenced by n values that are considerably less than 0.5. The process itself comprises three stages: (i) the diffusion of oil into the empty air-filled pores, (ii) the diffusion of oil into the bulk material (matrix), and (iii) the completion of the process through the volumetric changes of the sorbent during sorption. The exceptionally rapid sorption rate in the initial phase (within a few tens of seconds) is likely due to oil penetration into the highly interconnected pores. Concurrently, but at a slower rate, oil diffuses into less accessible pores and the solid polymeric walls.

In principle, two basic mechanisms for oil sorption into a foam can be considered. As discussed above, the first model group considers diffusion as the key sorption mechanism. The diffusion requires a chemical potential (a concentration gradient) to drive sorption processes. The second concept is based on the "sucking" of oil into the solid porous structures by capillary surface tension forces. In the latter, this

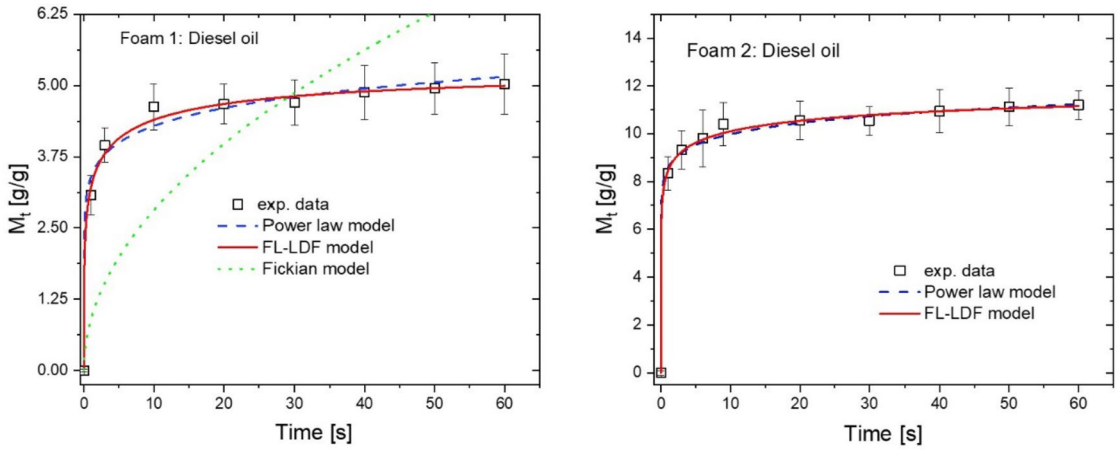

Fig. 7 Absorption capacity (M_t) of Foam 1(left) and Foam 2 (right) for Diesel oil compared with the Power law model (blue dashed) (left), FL-LDF model (red), and Fickian model (green dotted)

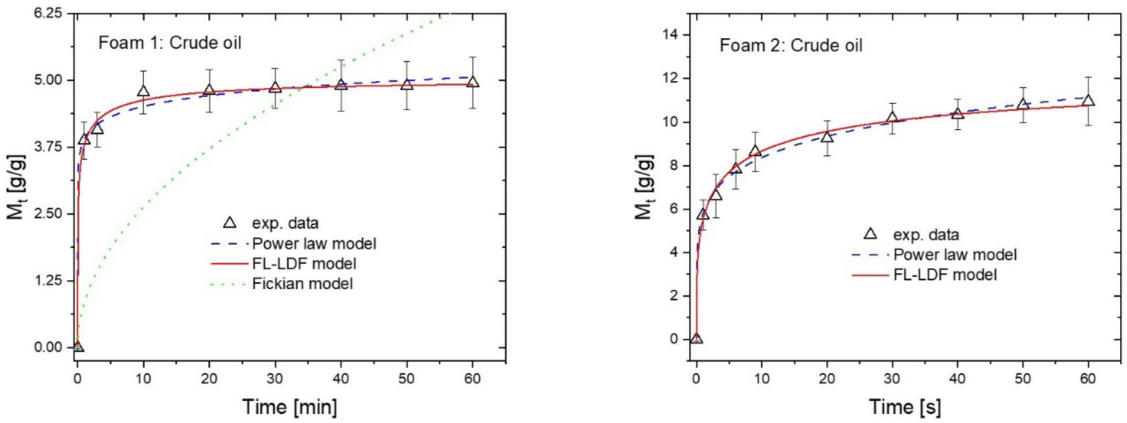

Fig. 8 Absorption capacity (M_t) of Foam 1(left) and Foam 2 (right) for crude compared with the Power law model (blue dashed) (left), FL-LDF model (red), and Fickian model (green dotted)

Table 1 Parameters of the FL-LDF and power law models for foam 1

Models/Parameters	Hexane	Diesel oil	Crude oil
$M_t = M_{max}[1 - \exp(-D\prime\, t^{\alpha})]$			
M_{max} [g/g]	4.53 (0.12)	4.83 (0.11)	5.11 (0.26)
D' [min^{-1}]	0.72 ((0.27)	0.95 (0.01)	1.41 (0.25)
α [-]	0.1 (0.02)	0.28 (0.01)	0.06 (0.02)
R^2	0.99992	0.99766	0.99947
$\frac{M_t}{M_\infty} = kt^n$			
k [(g/g).min^{-n}]	0.79 (0.04)	0.65 (0.03)	0.78 (0.03)
n [-]	0.05 (0.02)	0.1 (0.01)	0.28 (0.02)
R^2	0.99992	0.97457	0.99924

Table 2 Parameters of the FL-LDF and power law models for foam 2

Models/Parameters	Hexane	Diesel oil	Crude oil
$M_t = M_{max}[1 - \exp(-D\prime\, t^{\alpha})]$			
M_{max} [g/g]	8.2 (0.3)	12.5 (0.4)	12.2 (0.4)
D' [min^{-1}]	1.71 (0.41)	1.24 (0.52)	0.61 (0.08)
α [-]	0.25 (0.06)	0.21 (0.08)	0.32 (0.05)
R^2	0.99824	0.99952	0.99937
$\frac{M_t}{M_\infty} = kt^n$			
k [(g/g).min^{-n}]	0.82 (0.05)	0.68 (0.05)	0.48 (0.06)
n [-]	0.06 (0.02)	0.06 (0.01)	0.16 (0.03)
R^2	0.99942	0.99956	0.99946

process does not necessarily have to be considered as 'diffusion' because, per definition, diffusion is driven by a gradient in the Gibbs free energy, which may not always be the main driving force. For this reason, some authors explained absorption as a consequence of the capillary effect as the key mechanism of liquid penetration into empty (air-filled) porous materials [41, 42]. In this case, the driving force is the pressure gradient.

3.6 Water sorption

Water absorption is another parameter influencing the functionality of foams regarding their oil removal applications. The hydrophobic surface is needed to repel water and minimize water sorption. Hydrophobicity, like wettability by any liquid in general, is controlled by the chemical composition of the material and its surface morphology. Polyethylene is

inherently hydrophobic material due to its nonpolar character, having a contact angle for distilled water around 90°.

The foams investigated in this study show significantly different behavior if immersed in water or floating at the free water surface (Fig. 9). Foam 1 absorbed a relatively high amount of water, up to 1.5 g/g (mass of absorbed water/mass of a foam). This phenomenon is caused by the filling of large outer pores (immediate sorption) and continues by slight absorption during a more extended period due to capillary forces. Here, the sorption of water for one hour was investigated. Foams were floating on the free surface during the whole experiment.

On the other hand, Foam 2 showed a significantly lower water sorption capacity. After one hour, the maximum value was 0.14 g/g. This behavior is because of the very different morphology of Foam 2 in comparison to Foam 1. Foam 2 has a much smoother surface and smaller and uniform pores. A small amount of water is mainly absorbed in open pores on the surface, and it happens instantaneously, but further exposure to water does not lead to the addition of water sorption.

3.7 Reusability PE foams

The ability to reuse sorbents is a highly sought-after characteristic for all types, regardless of the recovery method employed. Foamy sorbents, in particular, are often retrieved for re-use through straightforward mechanical squeezing [43].

The foams with dimensions $1.5 \times 1.5 \times 0.1$ mm were immersed in oil for ten minutes, and then the oil was removed by squeezing using a syringe. Ten cycles were performed for each foam and oil (Fig. 10).

In contrast to vacuum removal, a portion of the oil becomes irreversibly trapped in the foam, making it impossible to release through simple squeezing. The amount of trapped oil depends on its viscosity, which varies between 10 and 20 wt% of the initially absorbed oil, and this is constant and does not change with an increased number of cycles. On the other hand, there is a significant difference between Foam 1 and Foam 2. Foam 1 shows significantly higher stability during cycling regarding the sorption capacity for all the oils. The comparison of the sorption capacities of Foam 1 between the first and the tenth sorption showed a decrease in the sorption capacity of 6.9, 6.2, and 6.4% for hexane diesel oil and crude oil, respectively. In the case of Foam 2, these decreases were 28.5, 35.0, and 28.05% for hexane, diesel, and crude oil, respectively. The recovery of Foam 2 from the deformed state after squeezing was also significantly slower than the same for Foam 1. Foam 1, due to crosslinking, exhibits much better elasticity and shape stability.

3.8 Mechanical properties

Dynamic mechanical analysis was performed (Fig. 11) in a broad temperature range from 150 to 100 °C. The highest temperature was kept around 10°C below the melting points of both foams.

Storage modulus for both cases is significantly higher than loss modulus, indicating good elastic properties. The decrease of the storage modulus for both samples with an increase in temperature is very slight, confirming the excellent stability of the fabricated foams for such a broad temperature range. Since during the intended potential application, the foam is expected to be immersed in the various solvents and then squeezed, the compression stress-strain curve was

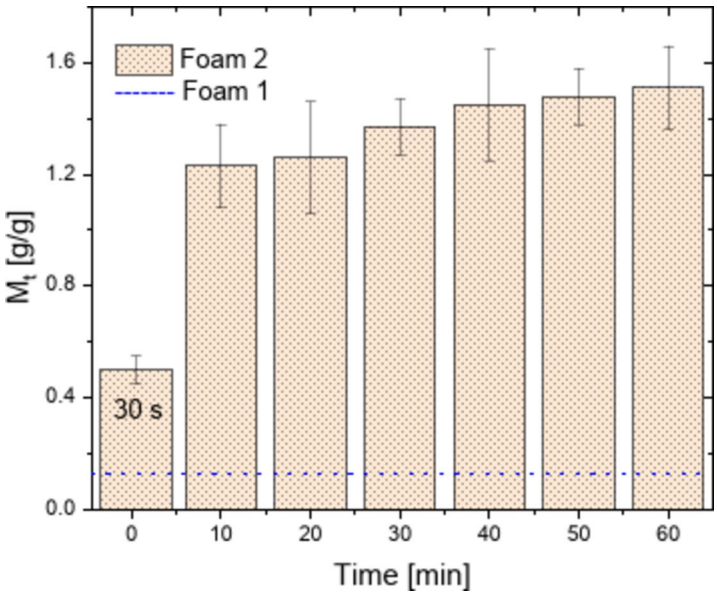

Fig. 9 Water sorption M_t [g/g] of Foam 1 and 2

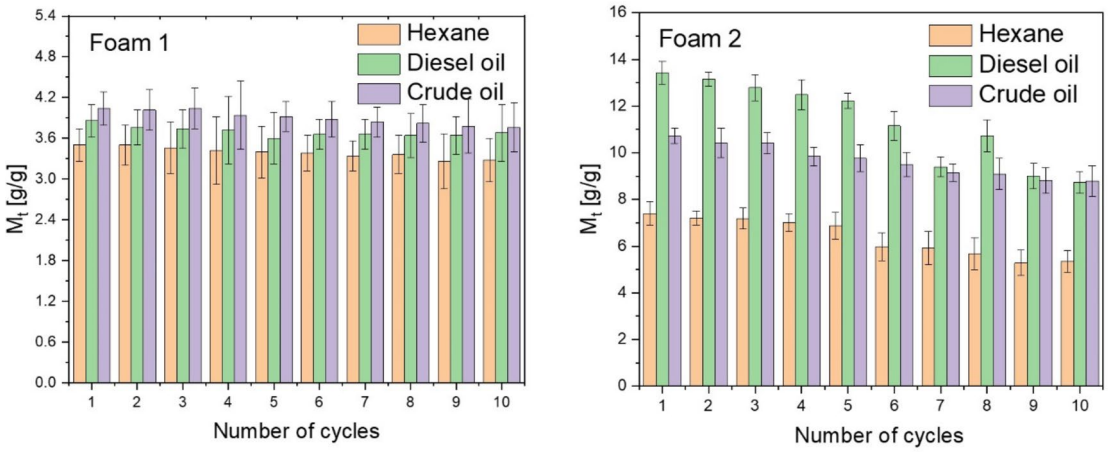

Fig. 10 Hexane, diesel oil, and crude oil sorption M_t [g/g] of Foam 1 and 2 for ten cycles

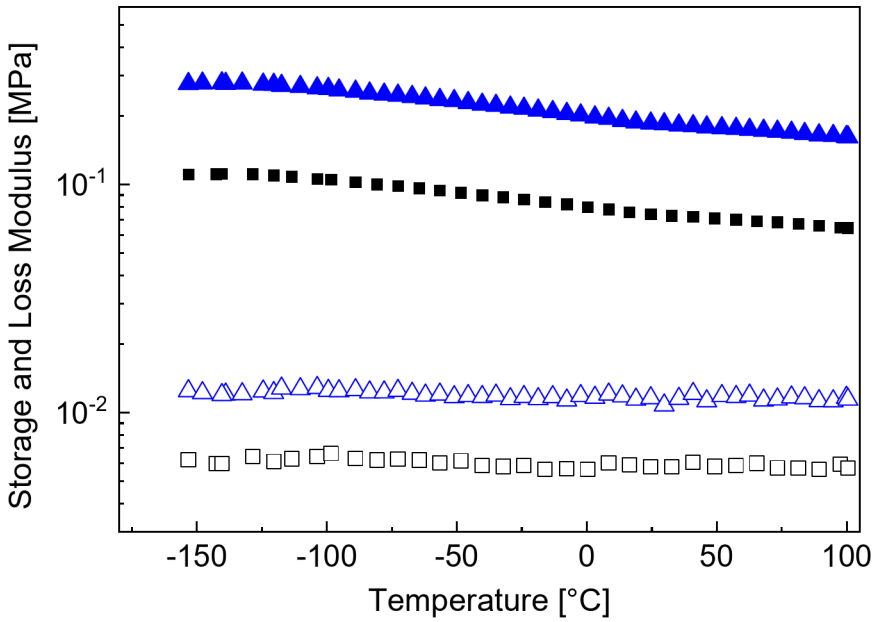

Fig. 11 Dependence of the storage (solid symbols) and loss (open symbols) modulus on the temperature. Foam 1 (triangles), Foam 2 (squares)

determined (Fig. 12). It was confirmed that compression comprising up to 60% of initial thickness leads to moderate compression stress (σ) increase up to 0.04 MPa or 0.06 MPa for Foam 1 and Foam 2, respectively. Young's modulus of both foams was determined by fitting the experimental data from the initial, linear deformation region (5%). The values were 0.325 MPs and 0.22 for Foam 1 and 2, respectively.

4 Conclusions

This study explores transforming LDPE waste into foamy structures that are applicable as free oil sorbents. The foam was prepared from LDPE waste using 1,1′-azobiscarbamide as the blowing agent. The structure of the foam was stabilized by crosslinking with dicumyl peroxide. The foam investigated in this study (Foam 1) was chosen based on the optimization of various components and processing conditions (S1). For comparison and to explore the potential of commercial LDPE foams, which were initially used for packaging, the second LDPE foam (Foam 2) was selected and tested under the same conditions as Foam 1.

Foam1 possesses around 75 vol% of pores (46 Vol.% open pores). It quickly absorbs various organic liquids (hexane, diesel oil, crude oil) in multiple cycles, whereas Foam 2 has a more porous structure with 96 vol% (89% of open pores). The organic liquids reported here as oil are hexane, diesel oil, and crude oil. Whereas the sorption capacity of Foam 1 was 4–5 g/g, depending on the type of oil, Foam 2 absorbed, while Foam 1 absorbed those oils in the range of 8–12 g/g. Foam 1 showed significantly better stability over multiple cycles and better mechanical performance.

The recycling of LDPE encounters several obstacles, including a lack of interest from converters, limited market

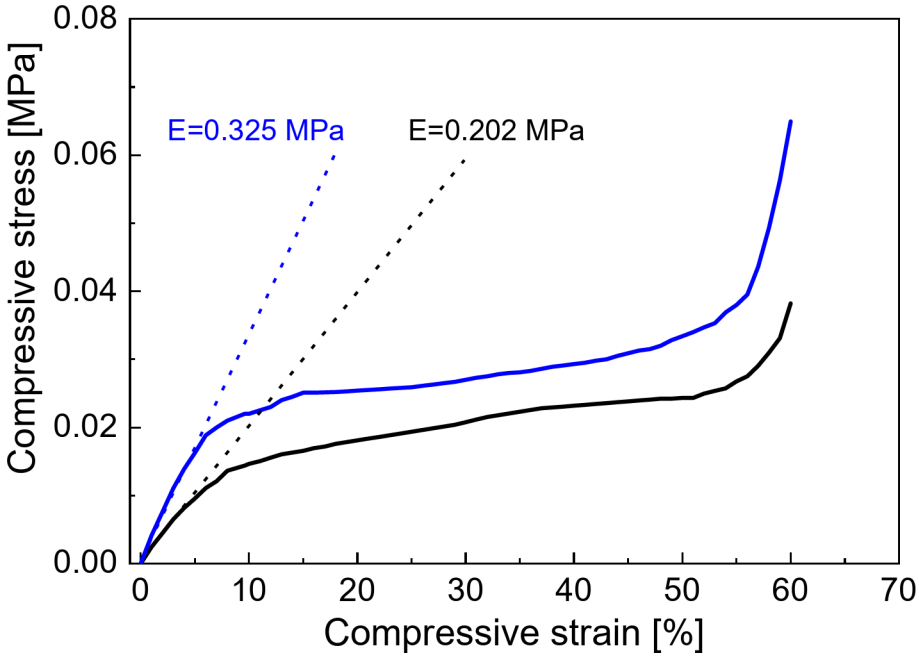

Fig. 12 The stress-strain curve in the compression mode for Foam 1 (blue solid line) and Foam 2 (black solid line). The dotted lines are tangents that calculate Young's modulus (E) in compression mode

demand for recycled products, higher costs associated with sorting and cleaning, diminished product quality, weakened mechanical properties, and inferior aesthetic performance compared to virgin LDPE. These challenges stem mainly from the fact that recycled LDPE is rarely suitable for its original intended use, especially in packaging. To overcome these issues and prolong the material's lifecycle, there is a pressing need to explore new applications for LDPE recyclates. One promising avenue is converting LDPE waste into foamy sorbents for water purification.

DMA characterized the mechanical properties of both foams over a broad range of temperature intervals from −150 to 100ºC. Both foams demonstrated significant mechanical stability within this range of temperatures. The stress-strain curve in the compression mode characterized the robustness of the foams. In addition, Young's modulus of both foams was determined by fitting the experimental within from the initial, linear deformation region (5%). The values were 0.325 MPs and 0.22 for Foam 1 and 2, respectively, showing significantly higher mechanical robustness of crosslinked foam.

This study shows the possibility of preparing foamy structures from recycled LDPE that can be applied to remove free oil spills. It follows that the transformation of low-cost polymeric waste recyclates can extend the material's lifespan for different applications. The conversion of LDPE waste into foamy sorbents for water purification is a promising application. One significant benefit of polyolefin-based materials is their environmentally friendly disposal at the end of their life cycle. Pyrolysis has emerged as the most efficient alternative to traditional landfilling. Unlike other materials, polyolefin-based sorbents are free of harmful elements like sulfur and nitrogen, which can release toxic byproducts during combustion and negatively affect the quality of pyrolysis outcomes. To further enhance the performance of foams, future research should focus on optimizing porosity by developing well-tuned open pores of the right size and ensuring sufficient mechanical stability under compression. This optimization will enable the foams to withstand multiple squeezing cycles, similar to conventional polyurethane or melamine formaldehyde foams. Achieving this may involve varying blowing and crosslinking agents and adjusting processing parameters like temperature and crosslinking duration.

Supplementary Information The online version contains supplementary material available at https://doi.org/10.1007/s42247-025-01024-9.

Acknowledgements This research was made possible by a grant from the Qatar National Research Fund under its GSRA (GSRA9- L-1-0520-22027) Research Program.
The authors (M.M., M.I., and A.M.) gratefully acknowledge the Ministry of Education, Youth and Sports of the Czech Republic - DKRVO (RP/CPS/2024-28/003). Furthermore, author F.M. would like to gratefully acknowledge the project IGA of TBU in Zlín, reg. No. IGA/FT/2024/007 for financial support.

Author contributions S.H: data collection, experimentation, draft preparation. M.M.: experimentation, data evaluation, draft preparation. Z.N.: experimentation, data evaluation. M.I.: experimentation. A.P.: experimentation. A.M.: data evaluation. F.M.: experimentation. G. McKay- supervision, reviewing and editing, validation. I. K.: conceptualisation, supervision, writing—reviewing and editing, validation. All authors have given approval to the final version of the manuscript.

Funding Open Access funding provided by the Qatar National Library.

Data availability Data will be made available on request.

Declarations

Conflict of interest The authors declare no competing interests.

Disclaimer The findings achieved herein are solely the responsibility of the authors.

References

1. Polyolefins, Market| Size, Share, Growth| 2023–2028. https://www.marketdataforecast.com/market-reports/polyolefins-market. Accessed 24 May 2023
2. 25 Jaw-Dropping Plastic Waste Statistics in 2023 - The Roundup. https://theroundup.org/plastic-waste-statistics/. Accessed 24 May 2023
3. Recycling of Plastics - Hanser Publications, https://www.hanserpublications.com/Products/634-recycling-of-plastics.aspx. Accessed 24 May 2023
4. T. Al-Gunaid, P. Sobolčiak, I. Chriaa, M. Karkri, M. Mrlik, M. Ilčíková, T. Sedláček, A. Popelka, I. Krupa, Phase change materials designed from Tetra Pak waste and paraffin wax as unique thermal energy storage systems. J. Energy Storage. **64**, 107173 (2023). https://doi.org/10.1016/J.EST.2023.107173
5. S. Hailan, P. Ghosh, P. Sobolciak, P. Kasak, A. Popelka, M. Ouederni, S. Adham, M. Chehimi, G. McKay, I. Krupa, Purification of colloidal oil in water emulsions by cationic adsorbent prepared from recycled polyethylene waste. Process Saf. Environ. Prot. **183**, 771–781 (2024). https://doi.org/10.1016/J.PSEP.2024.01.042
6. A.M.A. Pintor, V.J.P. Vilar, C.M.S. Botelho, R.A.R. Boaventura, Oil and grease removal from wastewaters: sorption treatment as an alternative to state-of-the-art technologies. A critical review. Chem. Eng. J. **297**, 229–255 (2016). https://doi.org/10.1016/J.CEJ.2016.03.121
7. J. Saleem, Z.K.B. Moghal, G. McKay, Up-cycling plastic waste into swellable super-sorbents. J. Hazard. Mater. **453**, 131356 (2023). https://doi.org/10.1016/J.JHAZMAT.2023.131356
8. L.M.T.M. Oliveira, J. Saleem, A. Bazargan, J.L.D.S. Duarte, G. McKay, L. Meili, Sorption as a rapidly response for oil spill accidents: A material and mechanistic approach. J Hazard Mater **407**, 124842 (2021). https://doi.org/10.1016/J.JHAZMAT.2020.124842
9. B.S. Rathi, P.S. Kumar, Application of adsorption process for effective removal of emerging contaminants from water and wastewater. Environ. Pollut. **280**, 116995 (2021). https://doi.org/10.1016/J.ENVPOL.2021.116995
10. S.-J. Choi, T.-H. Kwon, H. Im, D.-I. Moon, D.J. Baek, M.-L. Seol, J.P. Duarte, Y.-K. Choi, A polydimethylsiloxane (PDMS) sponge for the Selective Absorption of Oil from Water. ACS Appl. Mater. Interfaces. **3**, 4552–4556 (2011). https://doi.org/10.1021/am201352w
11. S.M. Hailan, D. Ponnamma, I. Krupa, The Separation of Oil/Water mixtures by modified melamine and polyurethane foams: a review. Polym. (Basel). **13** (2021). https://doi.org/10.3390/POLYM13234142
12. L. Vásquez, L. Campagnolo, A. Athanassiou, D. Fragouli, Expanded graphite-polyurethane foams for Water-Oil Filtration. ACS Appl. Mater. Interfaces. **11**, 30207–30217 (2019). https://doi.org/10.1021/acsami.9b07907
13. J. Pinto, A. Athanassiou, D. Fragouli, Surface modification of polymeric foams for oil spills remediation. J. Environ. Manage. **206**, 872–889 (2018). https://doi.org/10.1016/J.JENVMAN.2017.11.060
14. N.Y. Abu-Thabit, O.J. Uwaezuoke, M.H. Abu Elella, Superhydrophobic nanohybrid sponges for separation of oil/ water mixtures. Chemosphere. **294**, 133644 (2022). https://doi.org/10.1016/J.CHEMOSPHERE.2022.133644
15. S.M. Hailan, I. Krupa, G. McKay, Removal of oil spills from aqueous systems by polymer sorbents. Int. J. Environ. Sci. Technol. **2024**, 1–22 (2024). https://doi.org/10.1007/S13762-024-05959-0
16. I. Krupa, A. Mahmoud, P. Sobolciak, A. Popelka, M. Mrlik, A. Minarik, S. Gasmi, M. Ouederni, S. Adham, A novel alternative to free oil remediation and recovery: foamy absorbents designed from low molecular paraffinic waste. Sep. Purif. Technol. **302**, 122118 (2022). https://doi.org/10.1016/J.SEPPUR.2022.122118
17. B. Sun, J. Li, Y. Guo, H. Li, H.Y. Mi, B. Dong, C. Liu, C. Shen, Superhydrophobic UHMWPE foams with high mechanical robustness and durability fabricated by supercritical CO2Foaming. ACS Sustain. Chem. Eng. **9**, 12663–12673 (2021). https://doi.org/10.1021/acssuschemeng.1c04573
18. M. Su, Y. Pan, G. Zheng, C. Liu, C. Shen, X. Liu, An ultra-light, superhydrophobic and thermal insulation ultra-high molecular weight polyethylene foam. Polym. (Guildf). **218**, 123528 (2021). https://doi.org/10.1016/J.POLYMER.2021.123528
19. C. Nam, H. Li, G. Zhang, T.C.M. Chung, Petrogel: New Hydrocarbon (Oil) Absorbent based on Polyolefin polymers. Macromolecules. **49**, 5427–5437 (2016). https://doi.org/10.1021/acs.macromol.6b01244
20. C. Nam, G. Zhang, T.C.M. Chung, Polyolefin-based interpenetrating polymer network absorbent for crude oil entrapment and recovery in aqueous system. J. Hazard. Mater. **351**, 285–292 (2018). https://doi.org/10.1016/J.JHAZMAT.2018.03.004
21. C. Nam, H. Li, G. Zhang, L.R. Lutz, B. Nazari, R.H. Colby, T.C.M. Chung, Practical oil spill recovery by a combination of Polyolefin Absorbent and Mechanical Skimmer. ACS Sustain. Chem. Eng. **6**, 12036–12045 (2018). https://doi.org/10.1021/ACSSUSCHEMENG.8B02322
22. X. Sun, G. Wang, Z. Xu, J. Chai, A. Zhang, G. Zhao, S. Li, Y. Wang, H. Jiao, Microcellular foaming-derived strong ultra-high molecular weight polyethylene/high-density polyethylene foams for thermally insulating and oil-water separating applications. J. Environ. Chem. Eng. **12**, 113992 (2024). https://doi.org/10.1016/J.JECE.2024.113992
23. X. Sun, G. Wang, Z. Xu, Z. Wang, G. Zhao, Advanced fabrication of ultra-high molecular weight polyethylene/ graphite nanoplates foam for enhanced oil–water separation and thermal insulation via a novel omnidirectional gas escape barrier mechanism. Chem. Eng. J. **503**, 158360 (2025). https://doi.org/10.1016/J.CEJ.2024.158360

24. Z. Xue, Y. Cao, N. Liu, L. Feng, L. Jiang, Special wettable materials for oil/water separation. J. Mater. Chem. Mater. **2**, 2445–2460 (2014). https://doi.org/10.1039/C3TA13397D
25. C. Chen, D. Weng, A. Mahmood, S. Chen, J. Wang, Separation mechanism and construction of surfaces with special wettability for Oil/Water separation. ACS Appl. Mater. Interfaces. **11**, 11006–11027 (2019). https://doi.org/10.1021/acsami.9b01293
26. M.A. Hubbe, O.J. Rojas, M. Fingas, B.S. Gupta, Cellulosic substrates for removal of pollutants from aqueous systems: a review. 3. Spilled oil and emulsified organic liquids. Bioresources. **8**, 3038–3097 (2013). https://doi.org/10.15376/BIORES.8.2.3038-3097
27. Z. Xue, M. Liu, L. Jiang, Recent developments in polymeric superoleophobic surfaces. J. Polym. Sci. B Polym. Phys. **50**, 1209–1224 (2012). https://doi.org/10.1002/POLB.23115
28. A. Abdulkareem, A. Popelka, P. Sobolčiak, A. Tanvir, M. Ouederni, M.A. AlMaadeed, P. Kasak, S. Adham, I. Krupa, The Separation of Emulsified Water/Oil Mixtures through Adsorption on plasma-treated polyethylene powder. Mater. (Basel). **14**, 1 (2021). https://doi.org/10.3390/MA14051086
29. R.N. Wenzel, Resistance of solid surfaces to wetting by water. Ind. Eng. Chem. **28**, 988–994 (1936). https://doi.org/10.1021/ie50320a024
30. A.B.D. Cassie, S. Baxter, Wettability of porous surfaces. Trans. Faraday Soc. **40**, 546–551 (1944). https://doi.org/10.1039/TF9444000546
31. J. Pinto, A. Athanassiou, D. Fragouli, Effect of the porous structure of polymer foams on the remediation of oil spills. J. Phys. D Appl. Phys. **49**, 145601 (2016). https://doi.org/10.1088/0022-3727/49/14/145601
32. Zur Theorie der sogenannten Adsorption gelöster Stoffe - Lagergreen, S. (Bihang, A. K. Svenske Vet. Ak. Handl. 24, II. Nr. 4, S. 49; 1899; Z. physik. Ch. 32, 174–75; 1900.). Zeitschrift für Chemie und Industrie der Kolloide **2**:15 (1907) https://doi.org/10.1007/BF01501332/METRICS
33. Y.S. Ho, G. McKay, The kinetics of sorption of basic dyes from aqueous solution by sphagnum Moss peat. Can. J. Chem. Eng. **76**, 822–827 (1998). https://doi.org/10.1002/CJCE.5450760419
34. W.J. WeberJr, J.C. Morris, Kinetics of Adsorption on Carbon from Solution. J. Sanit. Eng. Div. **89**, 31–59 (1963). https://doi.org/10.1061/JSEDAI.0000430
35. M. Tanzifi, M.T. Yaraki, A.D. Kiadehi, S.H. Hosseini, M. Olazar, A.K. Bhati, S. Agarwal, V.K. Gupta, A. Kazemi, Adsorption of Amido Black 10B from aqueous solution using polyaniline/SiO2 nanocomposite: experimental investigation and artificial neural network modeling. J. Colloid Interface Sci. **510**, 246–261 (2018). https://doi.org/10.1016/J.JCIS.2017.09.055
36. S. Songsaeng, P. Thamyongkit, S. Poompradub, Natural rubber/reduced-graphene oxide composite materials: morphological and oil adsorption properties for treatment of oil spills. J. Adv. Res. **20**, 79–89 (2019). https://doi.org/10.1016/J.JARE.2019.05.007
37. M. Hubbe, S. Azizian, S. Douven, Implications of apparent pseudo-second-order adsorption kinetics onto cellulosic materials: a review. Bioresources. **14**, 7582–7626 (2019). https://doi.org/10.15376/BIORES.14.3.7582-7626
38. M. Khosravi, S. Azizian, A new kinetic model for absorption of oil spill by porous materials. Microporous Mesoporous Mater. **230**, 25–29 (2016). https://doi.org/10.1016/J.MICROMESO.2016.04.039
39. P.L. Ritger, N.A. Peppas, A simple equation for description of solute release I. Fickian and non-fickian release from non-swellable devices in the form of slabs, spheres, cylinders or discs. J. Controlled Release. **5**, 23–36 (1987). https://doi.org/10.1016/0168-3659(87)90034-4
40. P.L. Ritger, N.A. Peppas, A simple equation for description of solute release II. Fickian and anomalous release from swellable devices. J. Controlled Release. **5**, 37–42 (1987). https://doi.org/10.1016/0168-3659(87)90035-6
41. C.A. Carrillo, D. Saloni, L.A. Lucia, M.A. Hubbe, O.J. Rojas, Capillary flooding of wood with microemulsions from Winsor I systems. J Colloid Interface Sci **381**, 171–179 (2012). https://doi.org/10.1016/J.JCIS.2012.05.032
42. H.J.G. Diersch, V. Clausnitzer, V. Myrnyy, R. Rosati, M. Schmidt, H. Beruda, B.J. Ehrnsperger, R. Virgilio, Modeling unsaturated flow in absorbent swelling porous media: part 1. Theory Transp. Porous Media. **83**, 437–464 (2010). https://doi.org/10.1007/S11242-009-9454-6
43. S.M. Hailan, D. Ponnamma, I. Krupa, The Separation of Oil/Water mixtures by modified melamine and polyurethane foams. Rev. Polym. 2021. **13**, 4142 (2021). https://doi.org/10.3390/POLYM13234142